

An accurate measurement of PMT TTS based on the photoelectron spectrum*

HUANG Wei-Ping(黄卫平) TANG Ze-Bo(唐泽波) LI Cheng(李澄)¹⁾
JIANG Kun(江琨) ZHAO Xiao-Kun(赵晓坤) WANG Peng-Fei(王鹏飞)

State Key Laboratory of Particle Detection and Electronics, Department of Modern Physics,
University of Science and Technology of China, Hefei 230026, China

Abstract: The water Cherenkov detector array (WCDA) for the Large High Altitude Air Shower Observatory (LHAASO) will employ more than 3600 hemisphere 8-inch photomultiplier tubes (PMTs). Good time performance of the PMT, especially the transit time spread (TTS), is required for the WCDA. In order to meet the demand of the WCDA experiment, an accurate measurement of PMT TTS based on the photoelectron spectrum is studied. The method is appropriate for multi-photoelectrons and makes it possible to measure the TTS of different photoelectrons simultaneously. The TTS of different photoelectrons for a Hamamatsu R5912 PMT is tested with a specially designed divider circuit. The relationship between TTS and number of photoelectrons is also presented in this paper.

Key words: LHAASO, WCDA, PMT, single photoelectron spectrum, transit time spread

PACS: 29.40.Ka, 85.60.Ha **DOI:** 10.1088/1674-1137/39/6/066003

1 Introduction

The LHAASO project [1] is to be built in Sichuan province, China. The main scientific goals of LHAASO are searching for galactic cosmic ray origins by extensive spectroscopy investigations of gamma ray sources above 30 TeV, all sky survey for gamma ray sources at energies higher than 300 GeV and energy spectrum and composition measurements of cosmic rays over a wide range, covering knees with fixed energy scale and known fluxes for all species at the low energy end. To accomplish these tasks, the proposed project consists of four detector arrays: 1 km² extensive air shower array (KM2A), including electron detector (ED) and muon detector (MD), 90000 m² water Cherenkov detector array (WCDA), 5000 m² shower core detector array (SCDA) and wide field of view Cherenkov telescope array (WFCTA), as shown in Fig. 1 [2].

WCDA is a high-sensitivity gamma-ray and cosmic-ray detector. The main purpose of WCDA is to survey the northern sky for the very high energy (VHE) gamma ray sources. The WCDA consists of 4 square water ponds, arranged in a square with size 150 m×150 m. The depth of the pond is about 4.5 m. Each pond is divided into 900 cells sized 5 m×5 m, partitioned by black plastic curtains to prevent the penetration of light yielded

in neighboring cells. A PMT resides in the bottom of each cell, looking upward to collect Cherenkov light produced by charged particles produced in the air shower. It records the arrival time and the charge of pulses [3]. One candidate PMT used in WCDA is Hamamatsu R5912, whose properties are close to the requirement of WCDA.

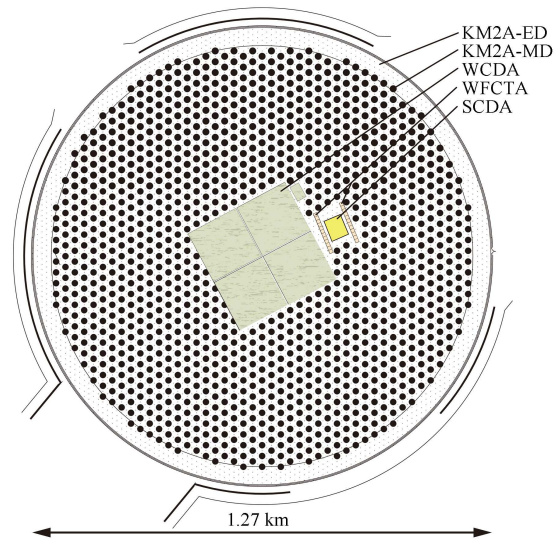


Fig. 1. Layout of LHAASO.

Received 5 September 2014

* Supported by Natural Science Foundation of China (11275196) and “Strategic Priority Program” of the Chinese Academy of Sciences (XDA03010100)

1) E-mail: licheng@ustc.edu.cn

©2015 Chinese Physical Society and the Institute of High Energy Physics of the Chinese Academy of Sciences and the Institute of Modern Physics of the Chinese Academy of Sciences and IOP Publishing Ltd

For a PMT in WCDA, the arrival time of Cherenkov light generated by an extensive air shower (EAS) is very short, depending on the depth of the shower front and the geometry of the cell. The EAS shower front is achieved according to the time reconstruction of various cell detectors. This reconstruction depends on the rise time and TTS of PMT in each cell detector. In consideration of reconstruction accuracy, the TTS (FWHM of transit time distribution) of PMT in WCDA must be less than 4.0 ns.

TTS is the deviation in transit time of photoelectrons between the photocathode and the anode. The spread of transit times in a PMT is caused by the following sources of time uncertainties:

- (1) Variation of the transit time of photoelectrons between the photocathode and the first dynode due to a different initial velocity and emission angles of photoelectrons;
- (2) Different transit times of photoelectrons emission from different points at the photocathode;
- (3) Time spread in the electron multiplication [4].

The TTS of a PMT is usually determined by using the single photoelectron counting technique, which calls for an exactly single photoelectron. The disadvantage of this method is to measure the TTS of single photoelectrons only. To measure the TTS of various photoelectrons, an accurate method using the photoelectron spectrum is studied. The method is appropriate for multi-photoelectrons and makes it possible to measure the TTS of different photoelectrons at the same time. Then the relationship of TTS and number of photoelectrons is studied.

An experimental setup designed for the TTS measurement will be shown in Section 2. The TTS measurement with a single photoelectron spectrum will be described in Section 3. The new method using multi-photoelectron spectrum to measure the TTS of different photoelectron will be shown in Section 4. Finally, the results of the measurements are summarized in Section 5.

2 Experimental setup

A PMT base is designed for the performance measurement of R5912, whose schematic is shown in Fig. 2. The voltage distribution between the cathode, focusing electrode and first dynode is adjusted to get a better time performance [5]. A typical pulse of PMT anode after a fast amplifier is shown in Fig. 3. The rise time of the pulse is about 4 ns and width is about 20 ns.

An experimental setup is built for TTS measurement, shown in Fig. 4. The output of laser (Hamamatsu PLP10-040C) has a 405 nm peak and 70 ps width. The dual timer (CAEN N93B) has two sync outputs and the

ADC (Lecroy 2249W) has a sensitivity of 0.25 pC. The width of ADC gate (Lecroy 2323A) is set to 300 ns. The PMT signal from anode is split into two. One is fed into the ADC to get the charge spectrum, and the other is fed into the discriminator connected to a TDC to get the time information.

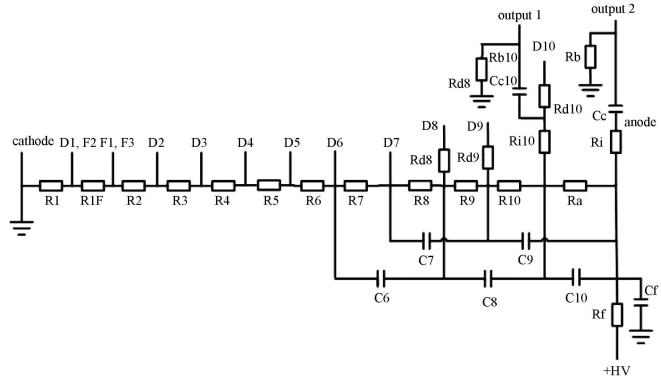


Fig. 2. Schematic of R5912 base.

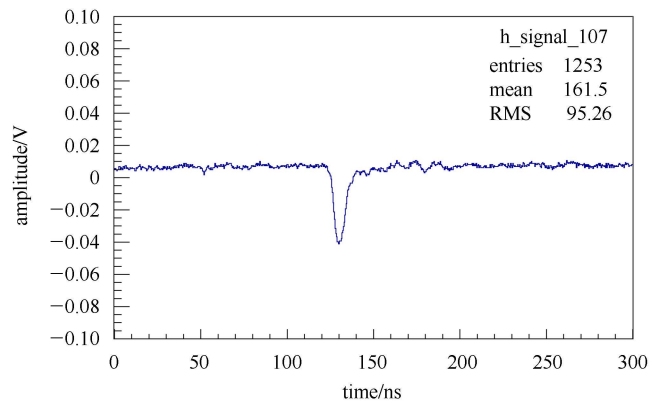


Fig. 3. A typical single photoelectron pulse of PMT anode with a fast amplifier.

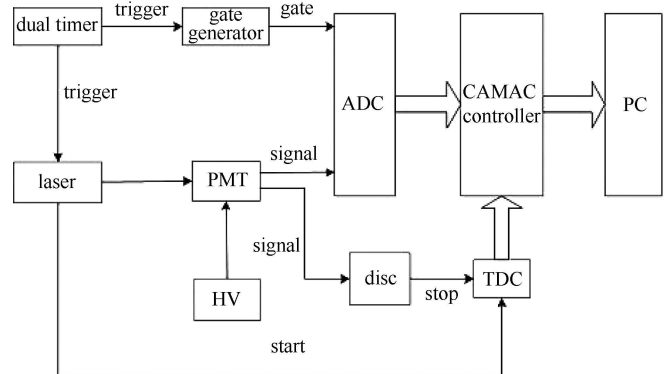


Fig. 4. Experimental setup for TTS measurement.

3 TTS measurement with SPE spectrum

The traditional method measuring TTS is the single photoelectron technique. This method needs an accurate SPE spectrum. The photoelectron spectrum is the convolution of charge distribution and pedestal, which can be described by the following distribution [6]:

$$S_{\text{ideal}}(x) = p(0, \lambda) \times \frac{1}{\sigma_0 \sqrt{2\pi}} e^{-\frac{(x-\mu_0)^2}{2\sigma_0^2}} + \sum_{n=1}^{\infty} p(n, \lambda) \times \frac{1}{\sigma \sqrt{2\pi n}} e^{-\frac{(x-n\mu)^2}{2n\sigma^2}}, \quad (1)$$

where λ is the mean number of photoelectrons collected by the first dynode, $p(n, \lambda)$ is the probability, n photoelectrons will be observed when their mean is λ , x is the variable charge, μ is the average charge at the PMT output when one electron is collected by the first dynode and σ is the corresponding standard deviation of the charge distribution.

In measurement, the single photoelectron spectrum can be determined by the following method: If the intensity of light reaching the PMT is such that 90 % of the time no signal is observed, the probability of seeing no photoelectron is $p(0, \lambda) = e^{-\lambda} = 0.9$, so $\lambda = 0.105$. The probability of seeing a single photoelectron is $p(1, \lambda) = \lambda e^{-\lambda} = 0.095$. Therefore, $p(n, \lambda) = 1 - 0.9 - 0.095 = 0.005$ when $n > 1$. Consequently, any signal observed above pedestal is dominated by single photoelectron events, since $p(1, \lambda)/p(n, \lambda) = 21$. So when $\lambda < 0.105$, the spectrum is an accurate SPE spectrum. A threshold is set to distinguish the pedestal and signal. Fig. 5 shows a SPE

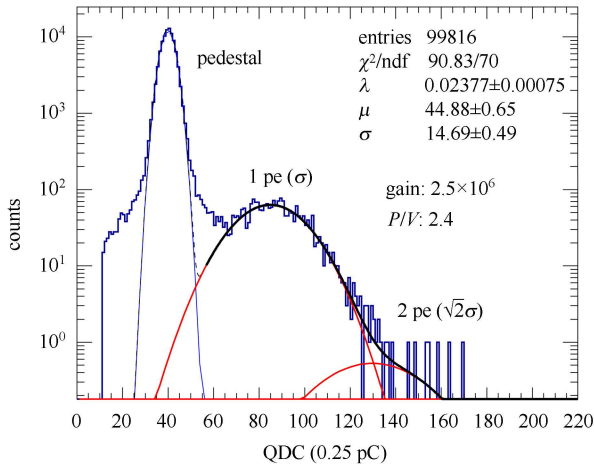


Fig. 5. A typical SPE spectrum at 1000 V. The leftmost Gaussian distribution is the pedestal and the right Gaussian distributions correspond to 1, 2 photoelectrons. The P/V is the peak-valley ratio of the SPE spectrum. The gain is calculated to be 2.6×10^6 . The λ is 0.023 to make $p(1, \lambda)/p(n, \lambda) = 86$.

spectrum at 1000 V with an amplifier[7]. The λ is 0.023 to make $p(1, \lambda)/p(n, \lambda) = 86$.

Since the used discriminator is a leading edge discriminator, with the same threshold, the TDC time has a jitter because of the different amplitude of the PMT pulse. Since there is strong correlation between the charge and amplitude, a time-charge ($T-Q$) correction is taken instead of the time-amplitude ($T-A$) correction, shown in Fig. 6. The relationship of TDC time and ADC charge is fit with a polynomial, then all the TDC time is corrected by this polynomial. Fig. 7 shows the distribution of transit time after $T-Q$ correction. The TTS is defined as the FWHM of this distribution.

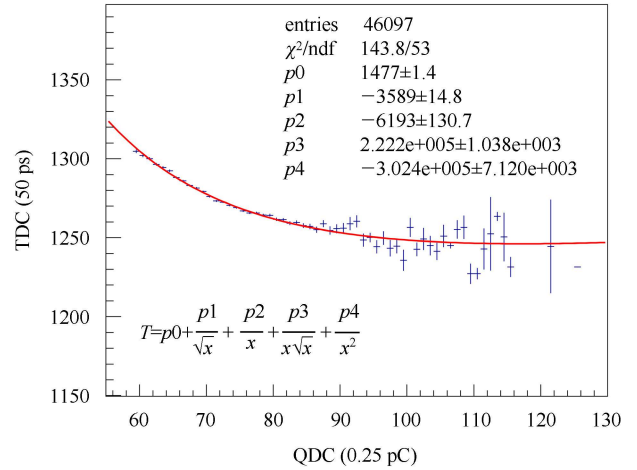


Fig. 6. $T-Q$ correction. In the charge range of the correction, the probability of single photoelectron is much higher than the one of multi-photoelectron to avoid its involvement.

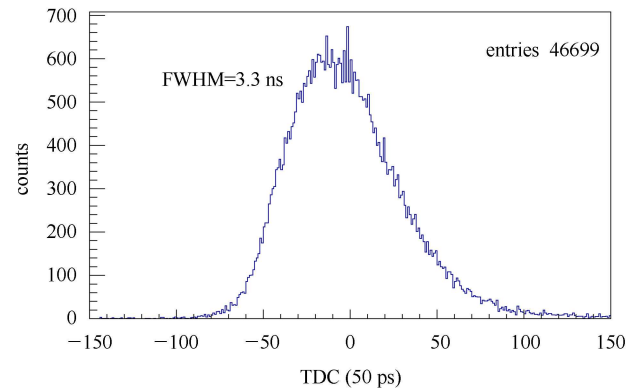


Fig. 7. TTS of a single photoelectron. The TTS is calculated to be 3.3 ns.

4 TTS measurement with multi-photoelectron spectrum

The single photoelectron technique is only for the TTS of single photoelectron. The number of photoelectrons received by each PMT in the WCDA is mainly 1,

2 and 3 photoelectrons. A new method is researched to measure the TTS of different photoelectrons. The method uses the multi-photoelectron spectrum to make it possible to separate the distribution of different photoelectrons. Fig. 8 shows the divided distribution with the multi-photoelectron spectrum, fitted with Eq. (1). Several charge (QDC) range cuts are adopted to separate the single, double, triple, four photoelectrons and more. Fig. 9 shows the ratio of different photoelectrons with charge. Then the QDC region is selected to be 60–70 ($Q1$) for single photoelectron, 85–95 ($Q2$) for double photoelectrons, 115–125 ($Q3$) for triple photoelectrons and 140–150 ($Q4$) for four photoelectrons. Fig. 10 shows the distribution of transit time of different photoelectrons in the QDC cut range after T - Q correction. The fraction of different photoelectrons and the TTS in different cut ranges are shown in Table 1. Since the TTS in each charge range includes the TTS of various photoelectrons, a correction is made to get the real TTS of different photoelectrons, the TTS correction follows the equation:

$$T_1'^2 = A_{11}T_1^2 + A_{12}T_2^2, \quad (2)$$

$$T_2'^2 = A_{21}T_1^2 + A_{22}T_2^2 + A_{23}T_3^2, \quad (3)$$

$$T_3'^2 = A_{32}T_2^2 + A_{33}T_3^2 + A_{34}T_4^2, \quad (4)$$

$$T_4'^2 = A_{43}T_3^2 + A_{44}T_4^2 + A_{45}T_5^2, \quad (5)$$

where T_n' is the measured TTS and T_n is the real TTS of different photoelectrons. A_{nm} is the normalized factor defined by the following formula:

$$A_{nm} = A'_{nm} / \sum A'_{nm}, \quad (6)$$

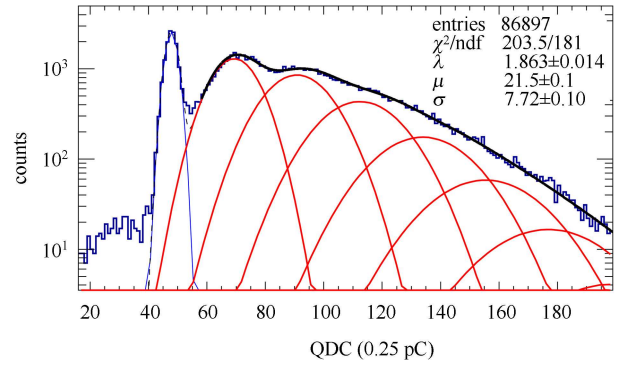


Fig. 8. Multi-photoelectron spectrum in TTS measurement.

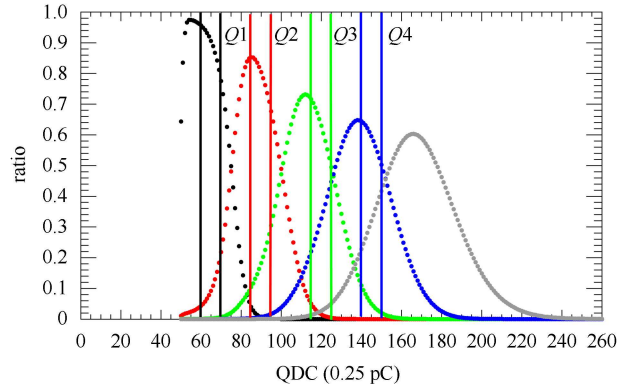


Fig. 9. The ratio of different photoelectrons with charge. The single photoelectron is determined from 60 to 70 channels, the double photoelectrons from 85 to 95, triple photoelectrons from 115 to 125 and the four photoelectrons from 140 to 150.

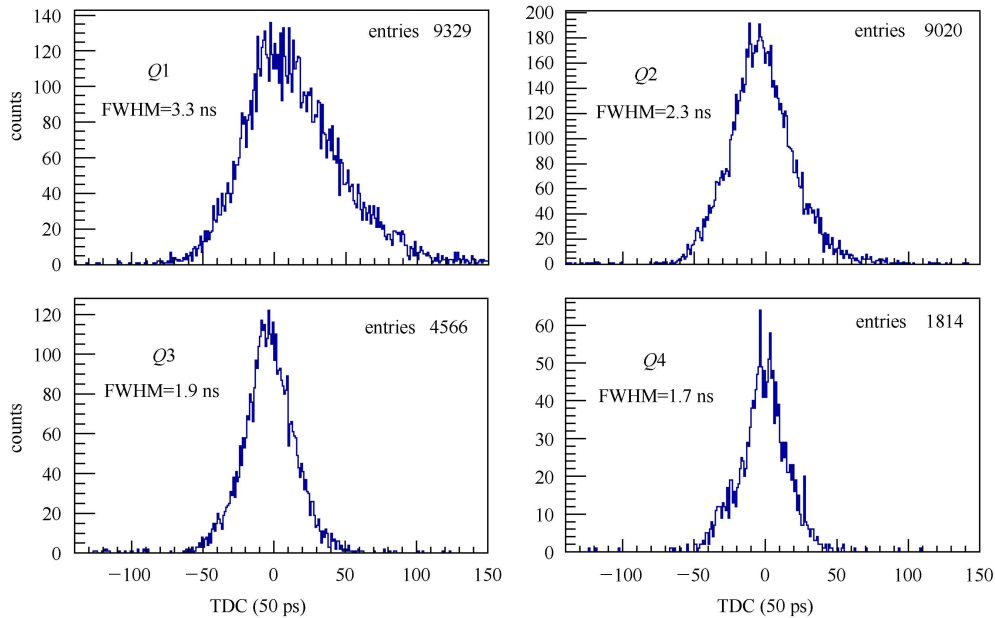


Fig. 10. The transit time distribution of different QDC regions.

Table 1. The fraction of different photoelectrons and TTS in QDC cut range.

QDC region	ratio of different photoelectrons	TTS before correction/ns	TTS after correction/ns
60–70	1 pe (88.9%) + 2 pe (10.9%)	3.3	3.4
85–95	1 pe (1.0%) + 2 pe (79.1%) + 3 pe (18.9%)	2.3	2.4
115–125	2 pe (3.5%) + 3 pe (62.8%) + 4 pe (32.3%)	1.9	2.0
140–150	3 pe (6.2%) + 4 pe (61.4%) + 5 pe (32.4%)	1.7	1.7

where A'_{nm} is the fraction of different photoelectrons in each charge cut range in Table 1, and it is assumed that $T_5 = 2T_4/\sqrt{5}$ to solve the equation. With the equation, the TTS of 1, 2, 3, 4 photoelectrons is calculated to be 3.4, 2.4, 2.0 and 1.7 ns respectively. Fig. 11 shows the fit between TTS and the number of photoelectron with the equation:

$$\text{TTS} = p_0 \times n^{p_1}, \quad (7)$$

where n is the number of photoelectrons. If p_0 and p_1 are fixed to 3.4 ns and 0.5, the chi-square value is $2.499/3$. So the TTS ratio of single photoelectron and n photoelectrons approximates \sqrt{n} .

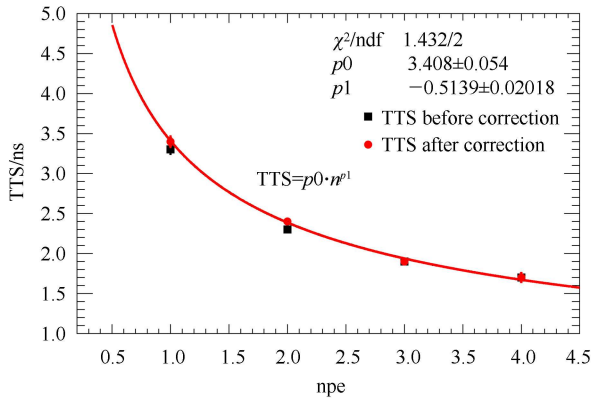


Fig. 11. The relationship of TTS and number of photoelectrons.

5 Summary

A new method based on the photoelectron spectrum to measure the TTS of different photoelectrons is stud-

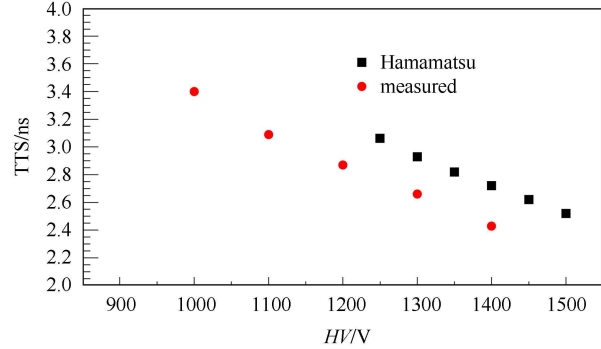


Fig. 12. TTS at different voltages, compared with manufacturer.

ied. The advantage of this method is that the TTS of different photoelectrons is achieved at the same time. After the correction, the TTS of single, double, triple and four photoelectrons is determined to 3.4 ns, 2.4 ns, 2.0 ns and 1.7 ns, which is in inverse proportion to the square root of the number of photoelectrons. TTS of single photoelectron is consistent with the single photoelectron method. TTS of single photoelectron at various high voltages is shown in Fig. 12, from which the measured value is less than the value provided by the manufacturer at the same voltage [8]. This difference is possibly caused by the PMT itself or the design of the PMT base. The method and technique will be used to batch test PMT performance for the LHAASO WCDA.

We gratefully acknowledge Prof. Zhen Cao, Prof. Huihai He, Prof. Zhiguo Yao, Dr. Mingjun Chen and other members of the LHAASO Collaboration of IHEP for their earnest support and help.

References

- 1 CAO Z et al. (LHAASO collaboration). Chinese Physics C, 2010, **34**(2): 249
- 2 CAO Z et al. (LHAASO collaboration). 2013, 33rd ICRC
- 3 YANG Qun-Yu et al. (LHAASO collaboration). Nuclear Instruments and Methods in Physics Research A, 2011, **644**: 11
- 4 Hamamatsu Photonics K K. Photomultiplier tubes basics and applications. Hamamatsu Photonics K K, 2006. 48–51
- 5 HUANG Wei-Ping, JIANG Kun, LI Cheng et al. Chin. Phys. C, 2013, **37**(3): 036001
- 6 Bellamy E H, Bellettini G, Budagov J et al. Nuclear Instruments and Methods in Physics Research A, 1994, **339**: 468
- 7 HAO Xin-Jun, LIU Shu-Bin, ZHAO Lei et al. Nuclear Electronics & Detection Technology, 2012, **32**(3): 352 (in Chinese)
- 8 <http://sales.hamamatsu.com/en/products/electron-tube-division/detectors/photomultiplier-tubes/part-r5912.php>